

Structural Biology
How to cite: *Angew. Chem. Int. Ed.* **2022**, *61*, e202112374

International Edition: doi.org/10.1002/anie.202112374

German Edition: doi.org/10.1002/ange.202112374

Structural Basis for Chaperone-Independent Ubiquitination of Tau Protein by Its E3 Ligase CHIP

Francesca Munari, Luca Mollica, Carlo Valente, Francesca Parolini, Elham Ataie Kachoe, Giorgio Arrigoni, Mariapina D'Onofrio, Stefano Capaldi,* and Michael Assfalg*

Abstract: The multi-site ubiquitination of Tau protein found in Alzheimer's disease filaments hints at the failed attempt of neurons to remove early toxic species. The ubiquitin-dependent degradation of Tau is regulated in vivo by the E3 ligase CHIP, a quality controller of the cell proteome dedicated to target misfolded proteins for degradation. In our study, by using site-resolved NMR, biochemical and computational methods, we elucidate the structural determinants underlying the molecular recognition between the ligase and its intrinsically disordered substrate. We reveal a multi-domain dynamic interaction that explains how CHIP can direct ubiquitination of Tau at multiple sites even in the absence of chaperones, including its typical partner Hsp70/Hsc70. Our findings thus provide mechanistic insight into the chaperone-independent engagement of a disordered protein by its E3 ligase.

concentration, localization, interactions and clearance.^[1] One of the key mechanisms governing protein turnover is the covalent attachment of ubiquitin and of its multimers (polyubiquitin chains) to target proteins via the formation of an isopeptide bond between the ubiquitin terminal glycine and substrate lysine side chains.^[2,3] Ubiquitination is carried out by the synergic activity of ubiquitin-activating (E1), ubiquitin-conjugating (E2), and ubiquitin ligase (E3) enzymes, the latter ensuring target specificity.^[2,4] Modification by Lys48-polyubiquitin is read by cells as a strong signal for substrate degradation by the proteasome.^[5] Ubiquitin-dependent protein degradation is crucial for the health of neurons, where protein remodeling is at the basis of specialized brain processes such as memory and learning, and synaptic plasticity.^[6] The age-dependent dysfunction of the mechanisms controlling protein clearance determines the accumulation of damaged and misfolded proteins within neurons.^[7] Indeed, the aberrant deposition of misfolded proteins represents a hallmark of multiple age-related neurodegenerative conditions such as Alzheimer's and Parkinson's disease.^[8]

In Alzheimer's disease (AD), the protein Tau, a microtubule-associated protein with a central role in axonal transport and neuronal functionality,^[9,10] converts into toxic amyloidogenic species and self-assembles into straight and paired helical filaments (SFs, PHFs) that accumulate within neurons.^[11] In PHFs, Tau is hyperphosphorylated and modified with both monoubiquitin and polyubiquitin mainly of the Lys48 type,^[12,13] suggesting an attempt of neurons to eliminate toxic species via the ubiquitin-proteasome system (UPS). A comprehensive mass-based profiling of pathological Tau in AD identified 17 specific ubiquitination sites, 16 of which are within the microtubule-binding domain (MBD)^[14] which is involved in the formation of the core of the PHFs.^[15] Notably, conjugation of ubiquitin to distinct lysine residues of Tau produces diverse effects on the protein aggregation mechanism.^[16,17] Despite the crucial role of ubiquitin in controlling Tau degradation and formation of filamentous aggregates, the regulatory and structural aspects of Tau ubiquitination remain elusive.

CHIP (carboxyl terminus of Hsp70 interacting protein), an E3 ubiquitin ligase of the RING/U-box type family, binds directly to Tau, promotes its ubiquitination both in vivo and in vitro,^[18–20] and is required for the in vivo ubiquitin-dependent degradation of phosphorylated Tau species.^[21] CHIP is known to mediate the ubiquitination of client proteins bound to Hsc70/Hsp70 or Hsp90 chaperones, promoting their degradation by the UPS or by the

Introduction

Maintaining a healthy proteome is pivotal for cellular functioning and involves the regulation of protein folding,

[*] Dr. F. Munari, Dr. F. Parolini, Dr. E. A. Kachoe, Dr. M. D'Onofrio, Dr. S. Capaldi, Prof. M. Assfalg
 Department of Biotechnology, University of Verona
 Strada Le Grazie 15, 37134 Verona (Italy)
 E-mail: stefano.capaldi@univr.it
 michael.assfalg@univr.it

Dr. L. Mollica, C. Valente
 Department of Medical Biotechnology and Translational Medicine,
 University of Milan
 Milan (Italy)

Prof. G. Arrigoni
 Department of Biomedical Sciences, University of Padova
 Padova (Italy)

Prof. G. Arrigoni
 Proteomics Center, University of Padova and Azienda Ospedaliera
 di Padova
 Padova (Italy)

© 2022 The Authors. Angewandte Chemie International Edition published by Wiley-VCH GmbH. This is an open access article under the terms of the Creative Commons Attribution Non-Commercial NoDerivs License, which permits use and distribution in any medium, provided the original work is properly cited, the use is non-commercial and no modifications or adaptations are made.

autophagy pathways,^[22] and preventing the accumulation of misfolded proteins in the cell.^[23–25] Specifically, a lysine clamp within a groove formed by the odd helices of the CHIP-TPR domain recruits members of the Hsp70 and Hsp90 families through the selective binding of their C-terminal (I/M)EEVD motif, thereby favoring the ubiquitination of the chaperone-bound proteins.^[26,27] On the other hand, CHIP can also ubiquitinate substrates independently of bound chaperones.^[26] Indeed we have recently shown that CHIP, in combination with the E2 enzyme Ubc13, and in the absence of Hsp(c)70, is able to catalyze the ubiquitination of the four-repeat region of Tau at multiple lysine residues,^[16] most of which have been found ubiquitinated also in Tau filaments isolated from the brain of AD patients.^[14]

Despite the central role of CHIP in the ubiquitin-dependent degradation of Tau, structural aspects concerning the recognition between the two proteins are still unknown. In the present work, by using high resolution NMR spectroscopy combined with computational and biochemical methods on both full-length proteins and shorter constructs, we provide insights into the recognition mechanism between Tau and CHIP, explaining the ability of this E3 ligase to operate in the absence of Hsc70. We show that the interaction is mainly directed by the repeat region of Tau which binds to the hairpin domain of CHIP. Additional contact sites were observed between the TPR domain of CHIP and N- and C-termini of Tau which might restrict the conformational flexibility of the protein complex. We found that the TPR domain is not required for CHIP to ubiquitinate Tau, thus explaining why Hsc70 is not essential for Tau ubiquitination and does not influence the ubiquitination pattern of Tau mediated by CHIP.

Results

Evidence has been provided to support the interaction between Tau and CHIP *in vivo* and *in vitro*,^[18,19,21] however detailed information on their recognition mechanism is currently lacking. In our work, we performed high resolution NMR experiments on ¹⁵N-labelled proteins, in the absence or presence of the partner, to unambiguously identify the binding interface between the two molecules. At first, we assessed the binding between the full-length human recombinant proteins, namely: 1) the Tau 2N4R isoform, an intrinsically disordered protein (IDP) of 441 residues that includes the two N-terminal inserts N1 and N2, the proline rich domains P1 and P2, and the four microtubule binding repeats (R1–R4) at the C-terminus (Figure 1A); 2) the 303-residue CHIP protein forming a homodimer in which each protomer has an N-terminal TPR domain containing the Hsp(c)70 binding site, a central helical hairpin, and a C-terminal U-box domain responsible for the binding to the E2 enzyme (Figure 1B). The two protomers associate through interactions established by the U-box and the helical hairpin, which displays an unusual asymmetric conformation in the crystal structure of the murine

protein^[27] but exhibits a high degree of structural flexibility in solution.^[28,29]

The ¹H-¹⁵N-HSQC spectrum of Tau 2N4R is shown in Figure 1C. The binding of CHIP caused strong attenuations of Tau NMR signals, which can be explained by the formation of a slowly tumbling complex. The plot of the intensity attenuations versus residue number (Figure 1D) revealed which regions of Tau contact the E3 ligase: the beginning of N1 (46–57) and the R3–R4 repeats up to the C-terminal end of the protein (307–441) exhibited the largest perturbations, followed by the P2–R1–R2 region (217–306) and the residues following N2 (100–115), which also experienced a considerable effect. The binding between full-length Tau and CHIP was of moderate affinity, as deduced from the NMR-derived dissociation constant, $K_d = 14 \mu\text{M}$ (Supporting Information Figure S1A). Since we employed a GST-tagged form of CHIP to confer greater solubility to the protein complex, we also reported a control experiment demonstrating that the GST alone had no effect on the NMR signals of Tau (Figure 1D). Notably, the binding profile of Tau 2N4R in complex with CHIP was very effectively reproduced by joining the intensity profiles of three shorter constructs of Tau, 1–152, 151–243, and 244–441, which were separately assayed for binding to CHIP (Figure 1E). Thus, these data indicate that distinct regions of Tau bind CHIP independently of each other.

To understand which part of CHIP was directly interacting with full-length Tau, NMR binding experiments were performed using the isolated domains of the E3 ligase. The U-box domain did not perturb Tau NMR signals (Figure 1F), thus ruling out its direct involvement in the complex formation. By contrast, the TPR domain induced a pronounced attenuation of signals for a number of residues belonging to the very N-terminal and C-terminal regions of Tau. The plot of the intensity attenuations allowed us to identify the stretches 46–57 and 413–428 (with $I/I_{\text{free}} < 0.5$) as specific TPR interacting regions (Figure 1F). The involvement of these motifs was also observed in the experiment with the entire CHIP protein (Figure 1D), while it was not detected on interaction with a CHIP mutant lacking the TPR domain (CHIP Δ TPR) (Figure 1G). The K_d value of 360 μM , determined by ITC (Supporting Information Figure S1B), indicated that the binding strength between the isolated TPR domain and Tau was lower than that of the full protein complex, in agreement with the fact that only part of the binding sites was engaged. The binding of full-length Tau to ¹⁵N-labelled TPR induced strong signal attenuations and small chemical shift perturbations (CSP) in the TPR spectra (Supporting Information Figure S2A, S2B). The analysis of CSP (Supporting Information Figure S2C) revealed that residues 64–66, 68, 70 in the N-terminal and 146, 148, 150, 152, 153 in the C-terminal of the TPR domain were the most perturbed upon binding. A clear signal perturbation in the region 62–71 was also observed upon addition of the C-terminal portion of Tau spanning residues 244–441 (Supporting Information Figure S2D). Taken together, these results suggest that the 413–428 stretch of Tau contacts directly the 64–70 region of TPR.

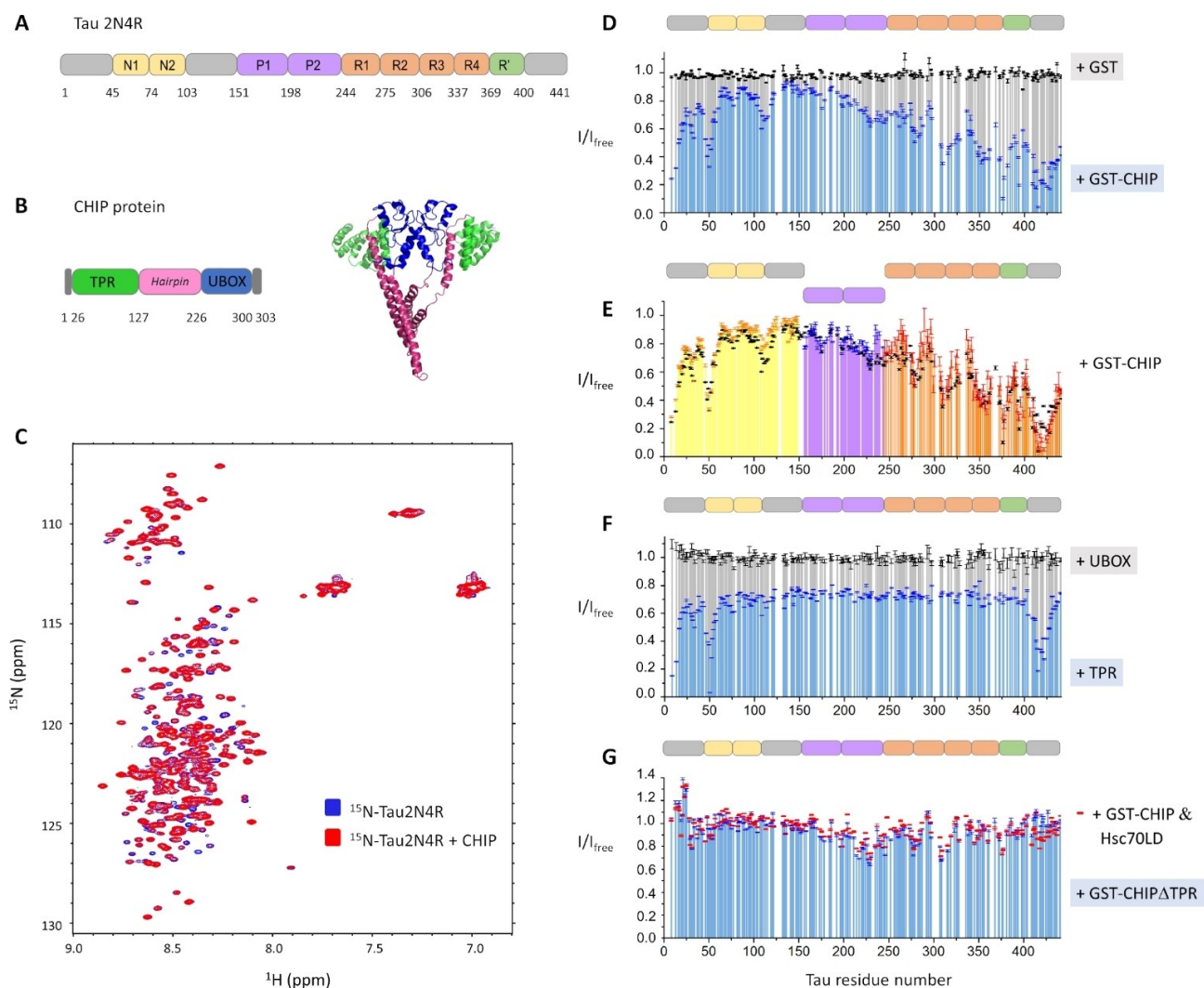


Figure 1. A) Domains organization of the Tau2N4R protein. B) Domain organization of CHIP. On the right, the X-ray structure from PDB 2c2v is shown.^[27] C)–G) NMR analysis of the Tau2N4R–CHIP interaction. C) Overlay of ^1H , ^{15}N -HSQC spectra of ^{15}N -Tau2N4R collected without (blue) and with (red) GST-CHIP at 3:1 molar ratio. D) NMR interaction profile of Tau2N4R with GST-CHIP (blue bars) or GST (gray bars), both at 3:1 molar ratio. E) NMR interaction profile of Tau1-152 (yellow bars), Tau151-243 (purple bars), Tau244-441 (orange bars), and Tau2N4R (black circles), all with GST-CHIP at 3:1 molar ratio. F) NMR interaction profile of Tau2N4R with TPR at 3:1 molar ratio (blue bars) or UBOX at 1.2:1 molar ratio (gray bars). G) NMR interaction profile of Tau2N4R with GST-CHIP Δ TPR at 3:1 molar ratio (blue bars) or GST-CHIP and Hsc70LD at 3:1:1 molar ratio (red sticks). In D–G, the plot of the peak intensity ratio (I/I_{free}) from ^1H , ^{15}N -HSQC spectra of ^{15}N -Tau constructs acquired alone (I_{free}) and in the presence of protein ligand (I), versus Tau sequence, is shown. Residues affected by severe signal overlap or low signal/noise were excluded from the analysis.

We then used molecular dynamics (MD) simulations and docking calculations to build a structural model of the Tau-TPR complex, using an ensemble of structures of the Tau405-430 peptide as a representative sequence containing the C-terminal TPR-interacting region. The calculation produced a bundle of low-energy structures of Tau405-430 centered within the cavity identified by the odd TPR helices (Figure 2A and Supporting Information Figure S3A, S3B).

The statistical analysis (see experimental methods and Figure S3C in Supporting Information) indicated that the Tau-TPR complex was specific and identified a low-energy hotspot in a cavity that had already been described as the binding site of Hsc70.^[26] From the analysis of the best lowest-energy ensemble of 200 structures, it appeared that

32% of Tau conformers populated the cavity, with Asp421 being positioned in proximity ($<10 \text{ \AA}$) of Lys30 or Lys95 (Figure 2B and Supporting Information Figure S3D). The latter are two key lysine residues that the TPR domain uses to specifically recognize the terminal carboxylates of the (I/M)EEVD motif of Hsp90(70) chaperones in a well characterized “two carboxylate clamp” mode.^[26,27,30] The absence of a C-terminal Asp in full-length Tau, as opposed to the caspase product Tau421D,^[30] explains its lower affinity to TPR.

Indeed, the Lid domain of Hsc70 (hereafter Hsc70LD), which includes the IEEVD motif, binds with submicromolar affinity to CHIP-TPR (Supporting Information Figure S1D) and it could prevent the interaction of TPR with Tau.

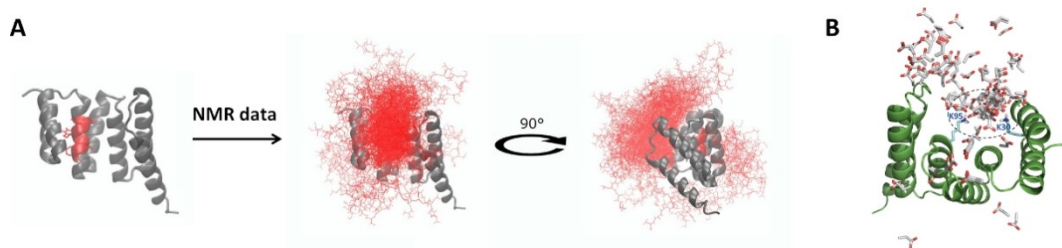


Figure 2. A) Data-driven rigid body docking flowchart from CSP data to Tau405-430-TPR complex. In the TPR structure (PDB ID: 4KBQ^[31]) reported as a ribbon on the left, the most perturbed region (63–72) according to NMR data, is highlighted in red. The result of rigid body docking of the TPR with Tau 405–430 peptides is reported on the right with the globular protein represented in gray ribbons and the Tau peptides as red stick structures B) Best lower-energy ensemble of 200 structures of Tau405-430-TPR complex, where TPR is shown as a green-colored ribbons and only Asp421 of Tau peptides is shown as red and grey colored sticks. Lys30 and Lys95 of TPR are shown as cyan and blue colored sticks.

To verify this hypothesis, we performed an NMR binding experiment between the full-length CHIP and Tau proteins in the presence of Hsc70LD. The NMR binding profile reported in Figure 1G indicated that no intensity attenuation occurred in the TPR-binding regions (46–57 and 413–428) of full-length Tau when Hsc70LD was present. Indeed, the same profile was obtained when CHIP Δ TPR was used (Figure 1G). The preference of TPR for the Lid domain of Hsc70 over Tau was confirmed by NMR experiments on ¹⁵N-labelled TPR. In the presence of Hsc70LD at 1:1 molar ratio, the HSQC spectrum of TPR changed with characteristic peaks shifts and broadening (Supporting Information Figure S2E). The co-presence of both Hsc70LD and full-length Tau at equimolar ratio (Supporting Information Figure S2F) produced spectral changes that were very similar to those obtained with Hsc70LD alone (Supporting Information Figure S2E) and different from those obtained with the sole Tau (Supporting Information Figure S2B).

The weak binding affinity measured in ITC experiments suggests that the TPR domain is not the part of CHIP that controls the interaction with Tau: indeed, the pull-down assay reported in Figure 3A shows that both CHIP and CHIP Δ TPR were able to bind full-length Tau in a comparable way. The experiment also showed that both CHIP variants efficiently pulled down the shorter Tau4RD construct, identifying the repeat region of Tau as the hot spot of the interaction, in agreement with previous biochemical data.^[19] With a K_d of 26 μ M (Supporting Information Figure S1C), the affinity of CHIP for Tau4RD was of the same order of magnitude as that between the two full-length proteins. The binding of Tau4RD to CHIP was cooperative, since almost no interaction occurred when a single repeat (R1, R2, R3 or R4) was used, while their combination (R2R3, R3R4, R1-R4) effectively promoted binding to CHIP (Figure 3B). Moreover, the binding decreased upon addition of NaCl in a concentration-dependent way (Figure 3C), indicating a significant contribution of electrostatic interactions to the formation of the complex. NMR data collected on ¹⁵N-labelled Tau4RD (Figure 3D,E) demonstrated that the isolated repeat domain associated with full-length CHIP in the same way as when incorporated in full-length Tau. No significant interaction was observed between Tau4RD and the isolated TPR domain, except for a contact

confined to the C-terminal part of the R4 repeat, between residue 351 and 361 (Figure 3F). On the other hand, Tau4RD was found to interact effectively with CHIP Δ TPR, exhibiting an NMR binding profile that well reproduced the pattern obtained with full-length CHIP. Three distinct binding sites in Tau4RD were identified: the region 263–293 between the R1 and R2 repeats, the region 295–330 between the R2 and R3 repeats and the stretch 341–361 in the R4 repeat (Figure 3F). The C-terminal of the R4 repeat appeared less involved in binding to CHIP Δ TPR compared to full-length CHIP (Figure 3E), in agreement with the absence of the contribution of the TPR domain.

Overall, our data indicate that the repeat region of Tau directs the interaction with CHIP, independently from the presence of the TPR domain. Since a significant contribution of the U-box domain was already ruled out (Figure 1F), we tested the direct interaction between the Tau repeats domain and the isolated helical hairpin domain of CHIP. The NMR binding experiment between ¹⁵N-labelled Tau4RD and a GST-tagged CHIP variant that includes only residues 130–221 (Figure 3G) confirmed the interaction between these protein domains and indicated that the three binding sites in Tau4RD were retained, with the 308–315 site in the R3 repeat displaying the largest signal perturbation. The effect on Tau signal intensity was here less pronounced, possibly due to the absence of the U-box dimer that results in a reduced size and faster tumbling of the complex.

As the data indicated that Tau could bind CHIP in the absence of the TPR domain, we tested whether the TPR was required for ubiquitination of Tau by CHIP. The ubiquitination assays reported in Figure 4A and Supporting Information Figure S4 showed that CHIP Δ TPR ubiquitinated Tau4RD in a comparable manner to the full-length ligase. Moreover, a comparable level of ubiquitination was obtained when full-length CHIP was employed together with the Hsc70 chaperone (Figure 4A), which we showed to effectively sequester the TPR domain. Indeed, MS fragmentation analysis of the ub-Tau4RD conjugate obtained by enzymatic reaction in the absence or presence of full-length Hsc70 identified the same pattern of ubiquitinated Tau lysine residues, including K259, K267, K274, K281, K290, K294, K298, K311, K317, K321, K331, K340, K353, and

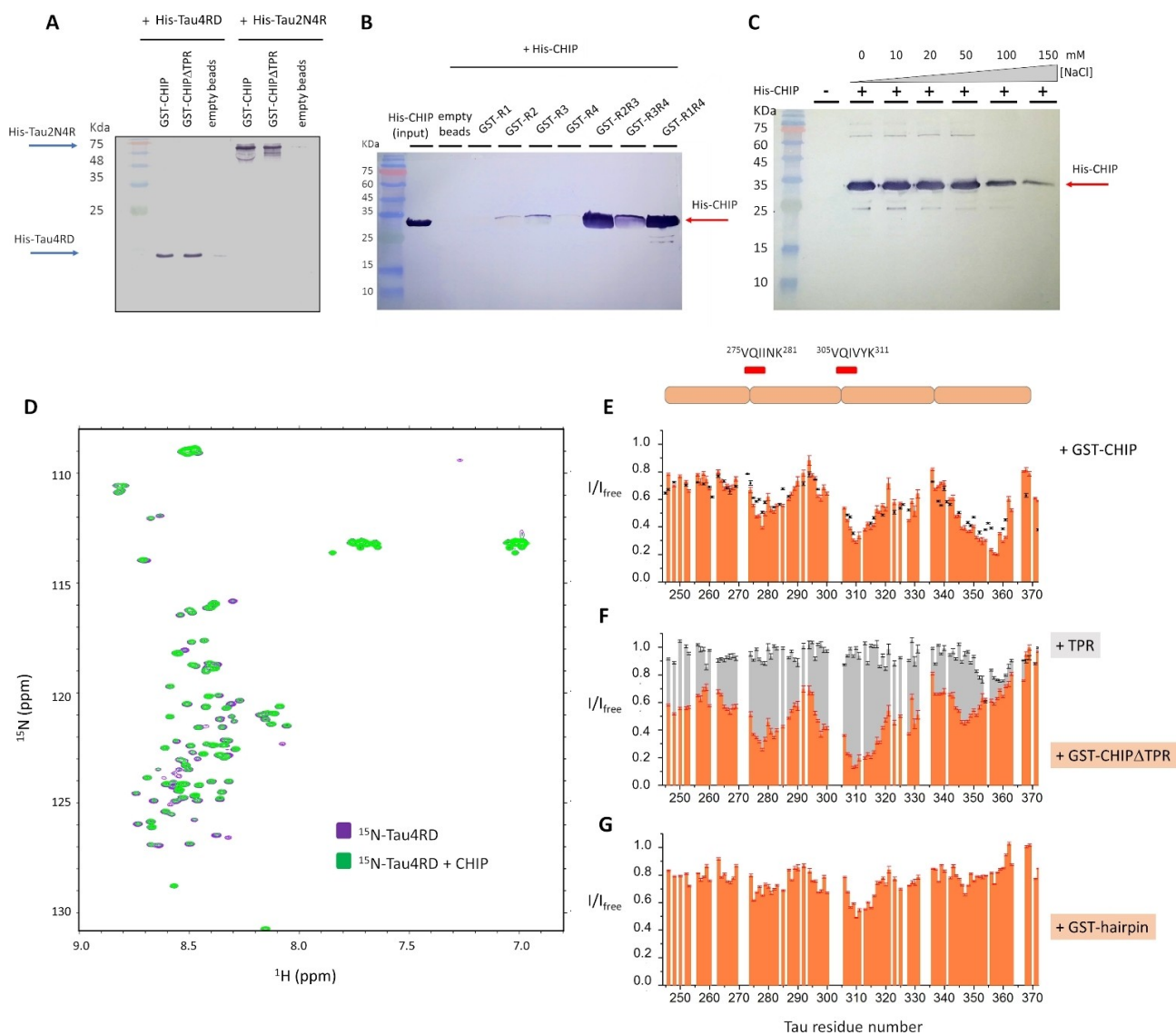


Figure 3. A) Immunoblot (IB) analysis of the binding between GST-CHIP/GST-CHIP Δ TPR and His-Tau4RD/His-Tau2N4R. B) IB analysis of the binding between His-CHIP and the GST-Tau repeats. C) IB analysis of the binding between His-CHIP and GST-Tau244–380 (R1–R4) at increasing NaCl concentration. In (A)–(C), the binding was probed by GST-pull down assay and the blots were developed with the anti-His mAb-HRP and the 4-chloro-1-naphthol reagent. D–G) NMR analysis of the Tau4RD–CHIP interaction. D) Overlay of ^1H , ^{15}N -HSQC spectra of ^{15}N -Tau4RD collected without (purple) and with (green) GST-CHIP at 1:1 molar ratio. E) NMR interaction profile of Tau4RD with GST-CHIP at 1:1 molar ratio (orange bars) in comparison with that of Tau2N4R with GST-CHIP at 3:1 molar ratio, restricted to region 244–372 (black circles). F) NMR interaction profile of Tau4RD with TPR at 1:1 molar ratio (gray bars) or GST- Δ TPR at 1:1 molar ratio (orange bars). G) NMR interaction profile of Tau4RD with GST-hairpin at 1:1 molar ratio (orange bars). In (E)–(G), the plot of the peak intensity ratio (I/I_{free}) from ^1H , ^{15}N -HSQC spectra of ^{15}N -Tau4RD acquired alone (I_{free}) and in the presence of protein ligand (I), versus Tau sequence is shown. Residues affected by severe signal overlap or low signal/noise were excluded from the analysis. On the top, the scheme of the Tau repeats organization is shown. The red bars above R2 and R3 identify the hexapeptides motifs PHF6* and PHF6 that promote Tau aggregation.

K370 (see Supporting Information excel and supplementary_MSdata files). Overall, these data clearly indicate that the TPR domain is not essential for the CHIP-mediated ubiquitination of Tau.

Discussion

The described findings provide novel insight into the molecular recognition between Tau and its ubiquitin ligase

CHIP. NMR binding experiments revealed that Tau associates with CHIP through distinct interaction sites: two stretches at the very N- and C-terminal regions (residues 46–57 and 413–428), the repeat domain and, to a lesser extent, part of the proline-rich region and the N2 domain (Figure 1). This multi-site recognition mode is made possible by the extraordinary flexibility of Tau, a long and intrinsically disordered polypeptide able to explore a large conformational space and offer multiple separate contact points for interaction with protein partners. Indeed, intrinsically dis-

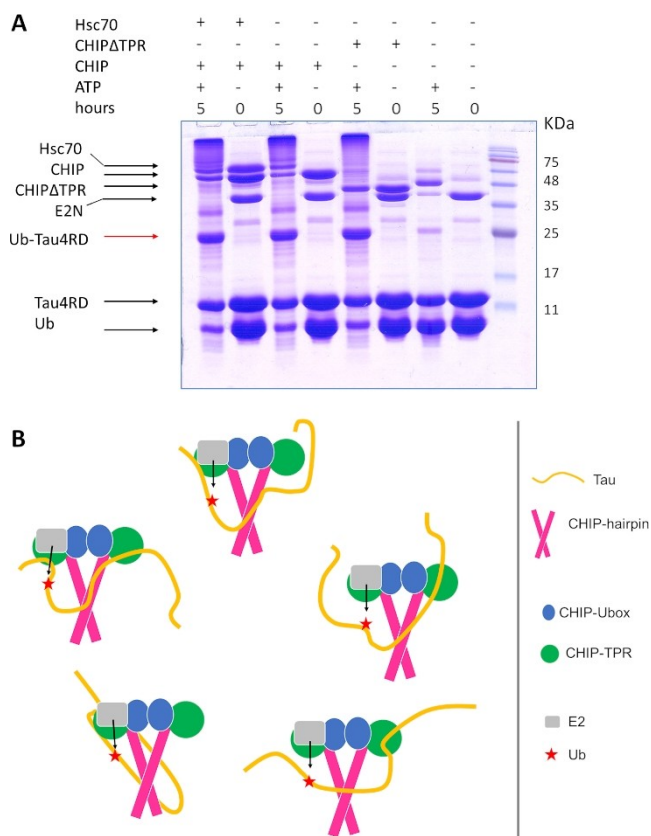


Figure 4. A) SDS-PAGE showing ubiquitination reaction of Tau4RD incubated at 37 °C for 5 hours with UBE1, E2N (hUbc13) and GST-tagged CHIP/CHIPΔTPR. B) Schematic model of the dynamic interaction between the E3 ligase CHIP and Tau protein and its chaperone-independent ubiquitination at multiple sites. Tau is represented as an orange line placed in multiple arrangements, whereby it can accept ubiquitin at different positions.

ordered proteins and regions (IDPs and IDRs) represent exceptional binding partners in regulating cellular pathways, being able to engage with interaction mechanisms not affordable by globular proteins.^[32–35]

Remarkably, the surface of Tau that engages CHIP is more complex than the one used to interact with other chaperone or co-chaperone proteins such as Hsp90,^[36] Hsc70,^[37] Hsp72^[37] or FKBP51.^[36] Indeed, in those cases, only part of the proline-rich domain and the repeat domain are deeply involved, while in the case of CHIP, additional recognition sites at the N- and C-terminal regions of Tau were identified and were shown to interact with the TPR domain (Figure 1). The NMR and computational analysis indicated that the C-terminal binding motif of Tau specifically occupies the TPR groove (Figure 1–2). Based on the determined binding affinities (Supporting Information Figure S1), it emerges that in physiological conditions the Tau-TPR interaction would not be competitive over that of Hsc70LD-TPR, but it could come to the fore in case of depletion of the cellular pool of active chaperones, as observed in neurodegenerative brains.^[38] Moreover, it was shown that other TPR-containing proteins, like FKBP51, can displace CHIP from binding to Hsp90, and their

elevated cellular levels, as found in AD brain, may increase the likelihood of CHIP to interact directly with protein targets.^[39]

Notably, we found that Tau exploits multiple sites of contact to engage CHIP, beyond the TPR, thus making this domain and co-bound chaperones not essential for the association with Tau. NMR data (Figure 1) clearly indicate that CHIP contacts a large portion of Tau, primarily localized to its repeat domain. The latter exhibits a higher content of hydrophobic residues, compared to the rest of the sequence, plunged in an otherwise positively charged surrounding. The analysis restricted to the isolated repeat domain (Figure 3) points out two hotspots of interaction with CHIP: the stretch 263–293 between the R1 and R2 repeats and, most importantly, the stretch 295–330 between the R2 and R3 repeats. The two regions include the hexapeptides motifs PHF6* (²⁷⁵VQIINK²⁸¹) and PHF6 (³⁰⁵VQIVYK³¹¹), which are considered crucial for the amyloid transition and pathological aggregation of Tau.^[40] Interestingly, the two motifs have also been implicated in mediating the interaction of the Tau repeat domain with Hsc70-Hsp70^[41] and Hsp90,^[42] chaperones that have the important role of burying aggregation-prone hydrophobic sites of IDPs or misfolded proteins. Thus, we envision that, beyond acting as a ubiquitin ligase, CHIP could also chaperone Tau by masking these hydrophobic sites and preventing their nucleation in pathological processes. Indeed, CHIP was found to decrease the elongation rate of filament formation for some Tau isoforms in thioflavin-based aggregation assays.^[43]

Importantly, the two contact regions 263–293 and 295–330 are retained in the binding between the isolated repeat domain of Tau and the CHIP mutant lacking the TPR or the short construct that only contains the helical hairpin domain (Figure 3). These data, together with evidence from the pull-down assay (Figure 3), clearly indicate that the repeat domain of Tau engages CHIP via the helical hairpin. This interaction is also observed in the context of full-length Tau in complex with CHIPΔTPR (Figure 1G), although the site-specific NMR signal intensity attenuation is less evident. The latter observation is partly due to the higher protein/ligand ratio, compared to the experiments with Tau4RD, and may also be attributed to competing intramolecular interactions between the acidic (Supporting Information Figure S5) N- and C-terminal regions and the repeat domain of Tau.^[44,45] In addition, the absence of anchors to TPR may increase the conformational dynamics of the repeat regions in the Tau–CHIP complex.

A computational energy-based analysis of possible binding sites for the Tau fragments 263–293, 295–330 and 341–361 on the surface of CHIP, subdivided in regions of 12 residues (Supporting Information methods and Table S1), showed an overall uniformity of binding energy values for all the tested CHIP fragments. This finding suggests that there is no unique binding site on CHIP and that the repeat domain of Tau may contact the hairpin domain at multiple points and with multiple orientations, in agreement with the flexible nature of an IDP. In the context of the full protein complex, the binding of the Tau N- and C-termini to the

TPR domain could be functional in facilitating the complex formation and restricting the conformations of the hairpin-bound Tau repeats. NMR data suggest that the U-box domain of CHIP is not directly involved in Tau recognition, although it might increase the overall affinity of the CHIP–Tau complex due to its involvement in CHIP dimerization. The disengagement of the U-box would be in line with its role in recruiting an E2 enzyme of the Ubc13^[27] or Ubch5^[19] type to ubiquitinate the substrate.

Conclusion

CHIP-mediated ubiquitination of Tau has crucial implications for Tau biology and pathology. We found that Tau associated with CHIP through a multivalent, cooperative interaction between three primary binding sites within the repeat domain of Tau and the helical hairpin of the ligase. Additional interactions were established between the Tau terminal regions and the CHIP-TPR domain. Computational analysis showed that the C-terminus of Tau preferentially interacted with a lysine clamp in the Hsc70-binding groove of TPR. Notably, the lack of TPR did not impair the binding of the Tau repeats to CHIP nor alter the ubiquitination pattern as determined by MS, although changes in the NMR intensity attenuation profile suggested an increase in fuzziness of the protein complex. The observed multi-site binding of Tau to the CHIP hairpin and the reported conformational dynamics of this domain in solution well explain how the E3 ligase can ubiquitinate the repeat region of Tau in multiple positions. These findings may provide the basis for the conception of molecular approaches aimed at modulating this protein–protein interaction to promote the ubiquitin-dependent clearance of Tau and ameliorate the progression of AD.

Acknowledgements

This work was supported by a grant from University of Verona (Progetto Ricerca di Base 2019 to F.M.), and by a grant from the University of Padova (BIRD189887/18 to G.A.). F.P. received a fellowship grant (Assegno di Ricerca) from the Department of Biotechnology of the University of Verona. Centro Piattaforme Tecnologiche (CPT) of the University of Verona is acknowledged for providing access to the NMR and ITC instruments. This work benefited from access to CERM/CIRMMP, an Instruct-ERIC center. Financial support was provided by Instruct-ERIC (PID 12742). Open Access Funding provided by Università degli Studi di Verona within the CRUI-CARE Agreement.

Conflict of Interest

The authors declare no conflict of interest.

Keywords: Alzheimer's Disease · CHIP E3 Ligase · NMR · Tau Protein · Ubiquitination

- [1] M. S. Hipp, P. Kasturi, F. U. Hartl, *Nat. Rev. Mol. Cell Biol.* **2019**, *20*, 421–435.
- [2] D. Komander, *Biochem. Soc. Trans.* **2009**, *37*, 937–953.
- [3] J.-F. Trempe, *Curr. Opin. Struct. Biol.* **2011**, *21*, 792–801.
- [4] C. M. Pickart, D. Fushman, *Curr. Opin. Chem. Biol.* **2004**, *8*, 610–616.
- [5] C. M. Pickart, *FASEB J.* **1997**, *11*, 1055–1066.
- [6] A. R. Dörrbaum, L. Kochen, J. D. Langer, E. M. Schuman, *eLife* **2018**, *7*, .
- [7] N. P. Dantuma, L. C. Bott, *Front. Mol. Neurosci.* **2014**, *7*, .
- [8] F. Chiti, C. M. Dobson, *Annu. Rev. Biochem.* **2017**, *86*, 27–68.
- [9] N. Hirokawa, *Curr. Opin. Cell Biol.* **1994**, *6*, 74–81.
- [10] A. Ebnet, R. Godemann, K. Stamer, S. Illenberger, B. Trinczek, E. Mandelkow, *J. Cell Biol.* **1998**, *143*, 777–794.
- [11] E. M. Mandelkow, E. Mandelkow, *Trends Cell Biol.* **1998**, *8*, 425–427.
- [12] H. Mori, J. Kondo, Y. Ihara, *Science* **1987**, *235*, 1641–1644.
- [13] D. Cripps, S. N. Thomas, Y. Jeng, F. Yang, P. Davies, A. J. Yang, *J. Biol. Chem.* **2006**, *281*, 10825–10838.
- [14] H. Wesseling, W. Mair, M. Kumar, C. N. Schlaffner, S. Tang, P. Beerepoot, B. Fatou, A. J. Guise, L. Cheng, S. Takeda, J. Muntel, M. S. Rotunno, S. Dujardin, P. Davies, K. S. Kosik, B. L. Miller, S. Berretta, J. C. Hedreen, L. T. Grinberg, W. W. Seeley, B. T. Hyman, H. Steen, J. A. Steen, *Cell* **2020**, *183*, 1699–1713.e13.
- [15] A. W. P. Fitzpatrick, B. Falcon, S. He, A. G. Murzin, G. Murshudov, H. J. Garringer, R. A. Crowther, B. Ghetti, M. Goedert, S. H. W. Scheres, *Nature* **2017**, *547*, 185–190.
- [16] F. Munari, C. G. Barracchia, C. Franchin, F. Parolini, S. Capaldi, A. Romeo, L. Bubacco, M. Assfalg, G. Arrigoni, M. D'Onofrio, *Angew. Chem. Int. Ed.* **2020**, *59*, 6607–6611; *Angew. Chem.* **2020**, *132*, 6669–6673.
- [17] F. Munari, C. G. Barracchia, F. Parolini, R. Tira, L. Bubacco, M. Assfalg, M. D'Onofrio, *IJMS* **2020**, *21*, 4400.
- [18] S. Hatakeyama, M. Matsumoto, T. Kamura, M. Murayama, D.-H. Chui, E. Planel, R. Takahashi, K. I. Nakayama, A. Takashima, *J. Neurochem.* **2004**, *91*, 299–307.
- [19] L. Petrucelli, D. Dickson, K. Kehoe, J. Taylor, H. Snyder, A. Grover, M. De Lucia, E. McGowan, J. Lewis, G. Prihar, J. Kim, W. H. Dillmann, S. E. Browne, A. Hall, R. Voellmy, Y. Tsuboi, T. M. Dawson, B. Wolozin, J. Hardy, M. Hutton, *Hum. Mol. Genet.* **2004**, *13*, 703–714.
- [20] J. H. Kim, J. Lee, W. H. Choi, S. Park, S. H. Park, J. H. Lee, S. M. Lim, J. Y. Mun, H.-S. Cho, D. Han, Y. H. Suh, M. J. Lee, *Chem. Sci.* **2021**, *12*, 5599–5610.
- [21] C. A. Dickey, M. Yue, W.-L. Lin, D. W. Dickson, J. H. Dunmore, W. C. Lee, C. Zehr, G. West, S. Cao, A. M. K. Clark, G. A. Caldwell, K. A. Caldwell, C. Eckman, C. Patterson, M. Hutton, L. Petrucelli, *J. Neurosci.* **2006**, *26*, 6985–6996.
- [22] V. Joshi, A. Amanullah, A. Upadhyay, R. Mishra, A. Kumar, A. Mishra, *Front. Mol. Neurosci.* **2016**, *9*, 93.
- [23] P. Connell, C. A. Ballinger, J. Jiang, Y. Wu, L. J. Thompson, J. Höhfeld, C. Patterson, *Nat. Cell Biol.* **2001**, *3*, 93–96.
- [24] J. Demand, S. Alberti, C. Patterson, J. Höhfeld, *Curr. Biol.* **2001**, *11*, 1569–1577.
- [25] M. Stankiewicz, R. Nikolay, V. Rybin, M. P. Mayer, *FEBS J.* **2010**, *277*, 3353–3367.
- [26] L. Wang, Y.-T. Liu, R. Hao, L. Chen, Z. Chang, H.-R. Wang, Z.-X. Wang, J.-W. Wu, *J. Biol. Chem.* **2011**, *286*, 15883–15894.
- [27] M. Zhang, M. Windheim, S. M. Roe, M. Pegg, P. Cohen, C. Prodromou, L. H. Pearl, *Mol. Cell* **2005**, *20*, 525–538.
- [28] Z. Xu, E. Kohli, K. I. Devlin, M. Bold, J. C. Nix, S. Misra, *BMC Struct. Biol.* **2008**, *8*, 26.

- [29] S.-B. Qian, L. Waldron, N. Choudhary, R. E. Klevit, W. J. Chazin, C. Patterson, *J. Biol. Chem.* **2009**, *284*, 26797–26802.
- [30] M. Ravalin, P. Theofilas, K. Basu, K. A. Opoku-Nsiah, V. A. Assimon, D. Medina-Cleghorn, Y.-F. Chen, M. F. Bohn, M. Arkin, L. T. Grinberg, C. S. Craik, J. E. Gestwicki, *Nat. Chem. Biol.* **2019**, *15*, 786–794.
- [31] H. Zhang, J. Amick, R. Chakravarti, S. Santarriaga, S. Schlanger, C. McGlone, M. Dare, J. C. Nix, K. M. Scaglione, D. J. Stuehr, S. Misra, R. C. Page, *Structure* **2015**, *23*, 472–482.
- [32] V. N. Uversky, *Chem. Soc. Rev.* **2011**, *40*, 1623–1634.
- [33] R. Bajaj, F. Munari, S. Becker, M. Zweckstetter, *J. Biol. Chem.* **2014**, *289*, 34620–34626.
- [34] H. Qi, S. Prabakaran, F.-X. Cantrelle, B. Chambraud, J. Gunawardena, G. Lippens, I. Landrieu, *J. Biol. Chem.* **2016**, *291*, 7742–7753.
- [35] J. Tolö, G. Taschenberger, K. Leite, M. A. Stahlberg, G. Spehlbrink, J. Kues, F. Munari, S. Capaldi, S. Becker, M. Zweckstetter, C. Dean, M. Bähr, S. Kügler, *Front. Mol. Neurosci.* **2018**, *11*, 49.
- [36] J. Oroz, B. J. Chang, P. Wysoczanski, C.-T. Lee, Á. Pérez-Lara, P. Chakraborty, R. V. Hofele, J. D. Baker, L. J. Blair, J. Biernat, H. Urlaub, E. Mandelkow, C. A. Dickey, M. Zweckstetter, *Nat. Commun.* **2018**, *9*, 4532.
- [37] U. K. Jinwal, E. Akoury, J. F. Abisambra, J. C. O’Leary, A. D. Thompson, L. J. Blair, Y. Jin, J. Bacon, B. A. Nordhues, M. Cockman, J. Zhang, P. Li, B. Zhang, S. Borysov, V. N. Uversky, J. Biernat, E. Mandelkow, J. E. Gestwicki, M. Zweckstetter, C. A. Dickey, *FASEB J.* **2013**, *27*, 1450–1459.
- [38] M. Brehme, C. Voisine, T. Rolland, S. Wachi, J. H. Soper, Y. Zhu, K. Orton, A. Villella, D. Garza, M. Vidal, H. Ge, R. I. Morimoto, *Cell Rep.* **2014**, *9*, 1135–1150.
- [39] L. J. Blair, B. A. Nordhues, S. E. Hill, K. M. Scaglione, J. C. O’Leary, S. N. Fontaine, L. Breydo, B. Zhang, P. Li, L. Wang, C. Cotman, H. L. Paulson, M. Muschol, V. N. Uversky, T. Klengel, E. B. Binder, R. Kaye, T. E. Golde, N. Berchtold, C. A. Dickey, *J. Clin. Invest.* **2013**, *123*, 4158–4169.
- [40] M. von Bergen, S. Barghorn, J. Biernat, E.-M. Mandelkow, E. Mandelkow, *Biochim. Biophys. Acta Mol. Basis Dis.* **2005**, *1739*, 158–166.
- [41] M. Sarkar, J. Kuret, G. Lee, *J. Neurosci. Res.* **2008**, *86*, 2763–2773.
- [42] G. E. Karagöz, A. M. S. Duarte, E. Akoury, H. Ippel, J. Biernat, T. Morán Luengo, M. Radli, T. Didenko, B. A. Nordhues, D. B. Veprintsev, C. A. Dickey, E. Mandelkow, M. Zweckstetter, R. Boelens, T. Madl, S. G. D. Rüdiger, *Cell* **2014**, *156*, 963–974.
- [43] S.-A. Mok, C. Condello, R. Freilich, A. Gillies, T. Arhar, J. Oroz, H. Kadavath, O. Julien, V. A. Assimon, J. N. Rauch, B. M. Dunyak, J. Lee, F. T. F. Tsai, M. R. Wilson, M. Zweckstetter, C. A. Dickey, J. E. Gestwicki, *Nat. Struct. Mol. Biol.* **2018**, *25*, 384–393.
- [44] S. Jeganathan, M. von Bergen, H. Brützlach, H.-J. Steinhoff, E. Mandelkow, *Biochemistry* **2006**, *45*, 2283–2293.
- [45] M. D. Mukrasch, S. Bibow, J. Korukottu, S. Jeganathan, J. Biernat, C. Griesinger, E. Mandelkow, M. Zweckstetter, *PLoS Biol.* **2009**, *7*, e34.

Manuscript received: September 11, 2021

Accepted manuscript online: February 2, 2022

Version of record online: February 18, 2022